1 **Technical Report – Methods: Automated Discovery of Functional Relationships in**
2 **Earth Systems Data**

3 **R. Reinecke[1,2], F. Pianosi[3,4], and T. Wagener[1]**

4 [1]Institute of Environmental Science and Geography, University of Potsdam, Potsdam, Germany

5 [2]Institute of Geography Johannes Gutenberg-University Mainz, Mainz, Germany

6 [3]Department of Civil Engineering, University of Bristol, Bristol, UK

7 [4]Cabot Institute, University of Bristol, Bristol, UK

8

9 Corresponding author: Robert Reinecke (reinecke@uni-mainz.de)

10 **Key Points:**

11 • Functional relationships capture how variables co-vary across spatial or temporal
12 domains.
13 • Here we present a new method for the automated diScovery Of fuNctionaAl
14 Relationships (SONAR).
15 • We test SONAR on model-derived datasets to identify functional relationships of
16 groundwater recharge simulations from global hydrological models with possible drivers.
17 • We compare SONAR to two established methods, CART (Classification and Regression
18 Trees) and CIT (Conditional Inference Trees), and find that SONAR produces smaller
19 trees and is more robust.

20 **Abstract**

21 Functional relationships capture how variables co-vary across specific spatial or temporal
22 domains. However, these relationships often take complex forms beyond linear, and they may
23 only hold for sub-sets of the domain. More problematically, it is often a priori unknown how
24 such sub-domains are defined. Here we present a new method called SONAR (diScovery Of
25 fuNctionAl Relationships) that enables the automated discovery of functional relationships in
26 large datasets. SONAR operates on existing unstructured data and is designed to be an
27 explorative tool for large datasets where manual search for functional relationships would be
28 impossible. We test the method on groundwater recharge outputs of several global hydrological
29 models to explore its usefulness and limitations. Further, we compare SONAR to the established
30 CART (Classification and Regression Trees) and CIT (Conditional Inference Trees) methods.
31 SONAR results in smaller trees with functional relationships in the leaf nodes instead of specific
32 classes or numbers. SONAR provides a robust and automated method for the exploration of
33 functional relationships.

34 **Plain Language Summary**

35 Vastly expanding datasets have the potential for incredible advancements in our understanding of
36 how different variables co-vary within Earth system dynamics. However, we lack adequate tools
37 to identify new relationships within such complex and high-dimensional datasets. Here we
38 developed a new method called SONAR that can automatically find relationships in large
39 datasets. We test the method on global simulations of groundwater recharge and find that it
40 produces smaller and more robust structured representations than existing methods. SONAR is
41 an exploratory tool that can help researchers discover relationships in complex datasets in the
42 Earth sciences and beyond.

43 **1 Introduction**

44 Earth system science relies on understanding functional relationships, which can be defined as
45 the co-variation of variables across space or and time that underpins our theoretical knowledge of
46 how the Earth works (Gnann et al., 2023a; L'vovich, 1979). For example, we find that
47 groundwater recharge across water limited domains co-varies with available precipitation
48 (MacDonald et al., 2021), or that changes in the co-variation of precipitation and runoff can
49 reflect system changes in response to drought (Peterson et al., 2021). To understand and
50 anticipate the evolving Earth system (Denissen et al., 2022), we require a quantitative
51 understanding of this co-variation. Not only is an understanding of such relationships important
52 for our scientific understanding, it also allows us to build adequate models and evaluate their
53 consistency with the Earth system dynamics we observe (Eker et al., 2018; Koster & Milly,
54 1997; Reichstein et al., 2019; Wagener et al., 2022). If finding functional relationships offers
55 such a high reward, how do we find them beyond manually looking for them – given that we can
56 rarely identify them through planned experiments at our scales of interest?

57 The dramatic increase in the size of datasets describing the structure and dynamics of the Earth
58 system offers huge opportunities for finding new relationships - if we have the tools to identify
59 them in vast and complex data. We have increasingly large satellite datasets; for example, the
60 new SWOT mission will send more than 1TB per day back to Earth, and the NASA Earth data
61 repository is estimated to grow to over 245 PB by 2025 (NASA, 2021). This does not even
62 include model outputs which add even more to the pile of data we have (e.g. Hoch et al. (2023)).

63 It will not be feasible to manually search through such datasets for functional relationships –
64 unless one makes very strong and thus limiting a priori assumptions about what we expect to
65 find. On the other hand, we struggle with imbalanced data, i.e. we often have unequal
66 distributions of relevant classes within the data (Bradter et al., 2022; Chawla et al., 2002; Kaur et
67 al., 2020), with human interference (Krabbenhoft et al., 2022), and with epistemic uncertainty
68 (Beven et al., 2018; Beven & Cloke, 2012). For example, Krabbenhoft et al. (2022) show that
69 global streamflow observations are significantly imbalanced and globally organized more by
70 national GDP than by hydrological considerations, thus providing limited information in dry
71 regions.

72 Earth systems datasets are a mixture of organized sampling (e.g. some remotely sensed
73 observations) and those that are not sampled in a strategic manner, but are rather samples of
74 opportunity (e.g. groundwater recharge estimates), thus requiring analysis methods that can work
75 with all samples. Methods that can work with generic input-output datasets have been called
76 sampling-free or data-agnostic methods (Pianosi & Wagener, 2018; Sheikholeslami & Razavi,
77 2020). Further, if methods require no manual parameter tuning, we call them parameter-free
78 (Saltelli et al., 2021). This is another advantageous feature of a method given that parameter
79 tuning can be different if very heterogenous and imbalanced datasets are studied. Both properties
80 would be beneficial for the automated exploration of functional relationships in Earth system
81 data.

82 Earth system processes are driven by different factors across space and time scales (Pattee,
83 1972), vary along gradients (Lesk et al., 2021), and exhibit thresholds (Zehe & Sivapalan, 2009).
84 Thus, an automated method should also be able to identify and represent relationships in a
85 hierarchical manner to represent the diversity in subdomains of the data. In the past, tree-like
86 algorithms such as CART (Classification and Regression Trees) (Breiman et al., 2017) and CIT
87 (Conditional Inference Trees) (Hothorn et al., 2006) and other similar implementations (Loh,
88 2014) have been used to find hierarchical structure in Earth system data (e.g., Messager et al.
89 (2021), Almeida et al. (2017)). While these algorithms have initially been built for classification
90 and regression, they also provide information about dominant controls. In fact, the point at which
91 the data are split into subtrees reveals the underlying structure of the data and the dominant
92 controls that separate sub-domains. However, these data-based strategies can show limited
93 robustness and can provide splits at non-physical boundaries rendering their interpretation
94 difficult (Sarailidis et al., 2023).

95 Addressing the robustness problem, ensemble methods such as random forest (Breiman, 2001)
96 can identify dominant controls through factor importance (Antoniadis et al., 2021), while others
97 have used multivariate adaptive regression splines (MARS) (Friedman, 1991) to find more
98 complex relationships (e.g., Conoscenti et al. (2015)). However, such approaches can be difficult
99 to interpret or even visualize. While visual inspection remains powerful in identifying complex
100 variable interactions – especially if we do not know what kind of interaction we might expect
101 (Puy et al., 2022; Wagener & Kollat, 2007). Similarly, machine learning has led to approaches
102 that learn functional relationships (Shrestha et al., 2009), and explainable AI strategies are
103 advancing rapidly (Jiang et al., 2022).

104 Here we present an automated method for the diScovery Of fuNctionAl Relationships
105 (SONAR) that combines data agnosticism, interpretability, and the identification of hierarchical
106 controls, in a parameter-free algorithm. What distinguishes SONAR from other existing methods
107 is that the automatic search yields a tree that separates the search domain in a hierarchical
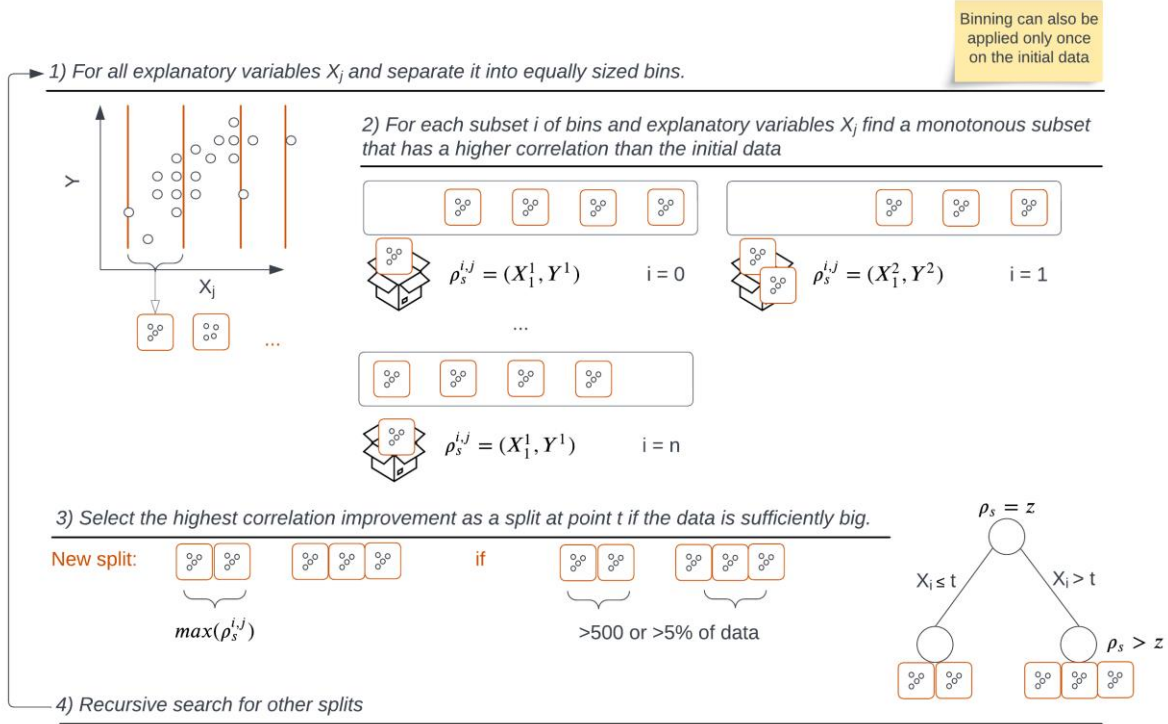
108   manner and uncovers possible functional relationships. To our knowledge, no method exists that
109   can automatically separate data in a hierarchical manner to show functional relationships.
110   SONAR is tested here on a large groundwater recharge dataset from eight global hydrological
111   models.

112   Groundwater recharge is an example of a hydrological process (see supplement for definition)
113   which remains highly uncertain on the global scale as hydrological models disagree largely in the
114   functional relationships they produce (Berghuijs et al., 2022; Reinecke et al., 2021; West et al.,
115   2023). It is unclear why exactly the models disagree and how it relates to differences in
116   assumptions made about how hydrologic systems work. However, one can clearly trace patterns
117   of different recharge behavior for different climatic zones across the globe (Fig. S1). Here we
118   test whether SONAR can be used to analyze synthetic (noise-free) datasets produced by
119   hydrological models and identify different functional relationships in different sub-domains (e.g.
120   climatic regions); and how its results compare with established strategies.

121   **2 Materials and Methods**

122   2.1 Automated discovery of functional relationships

123   SONAR works similarly to other tree-based approaches such as CART (Breiman et al., 2017).
124   However, SONAR is not built to solve a classification or a regression problem but to find
125   functional relationships while making no prior assumption about the type of relationship beyond
126   a choice of correlation metric (that can be varied; in the following we use the spearman rank
127   correlation). The algorithm works as follows (Fig. 1). It searches recursively for the best possible
128   split within the dataset. On each split SONAR determines which binary separation of an
129   explanatory variable (e.g., amount of precipitation above or below a certain threshold) would
130   increase the correlation between an explanatory variable (e.g., aridity index, or precipitation
131   amount again) and the variable under investigation (e.g., groundwater recharge). SONAR
132   searches for possible splits based on equally sized bins to reduce the search space into
133   manageable pieces. However, the correlations are always calculated on the original data and not
134   the bins. SONAR tests all possible splits based on different subsets of the bins (Fig. 1) from
135   small to large values of the explanatory variables (for description of alternatives see
136   Supplement). SONAR can also handle categorical variables, in which case the split is based on
137   whether the data belong to a certain category or not. With each split SONAR searches for an
138   increase in correlation. SONAR produces binary trees and for each split at least one side (the left
139   or right subtree) needs to increase in correlation otherwise the algorithm stops (Fig. 1). Requiring
140   an increase for both sides would yield a less robust algorithm given that we want to distinguish
141   sub-domains in which functional relationships exists from those where this is not the case. To
142   ensure that SONAR does not select very small subspaces a split requires each subspace to have
143   at least 500 data points or 5% of the data of the parent node – depending on the dataset used.
144   This value can be changed and limits the parameter-free property of the approach.
145   Importantly, each leaf node ends up containing a relationship and not only a particular class
146   (compared to classification trees) or value (compared to regression trees). Each leaf thus contains
147   a subset of the original data points for the particular subdomain. SONAR then derives a
148   functional relationship in the following way: the data in each leaf node are divided into 10
149   equally-sized bins and a line is added that connects the medians across the bins to describe the
150   functional relationship.

1) For all explanatory variables X_j and separate it into equally sized bins.

Binning can also be applied only once on the initial data

2) For each subset i of bins and explanatory variables X_j find a monotonous subset that has a higher correlation than the initial data

$\rho_s^{i,j} = (X_1^1, Y^1)$ i = 0

$\rho_s^{i,j} = (X_1^2, Y^2)$ i = 1

...

$\rho_s^{i,j} = (X_1^1, Y^1)$ i = n

3) Select the highest correlation improvement as a split at point t if the data is sufficiently big.

New split: if

$max(\rho_s^{i,j})$ >500 or >5% of data

$\rho_s = z$

$X_i \leq t$ $X_i > t$

$\rho_s > z$

4) Recursive search for other splits

Figure 1. Visual representation of the SONAR algorithm and its major workflow components. Y denotes the variable we are searching dominant controls for in the set of explanatory variables Xj. ps is the Spearman Rank correlation and z the highest ps of the node above a split (this can also be the root node).

2.2 Approaches related to our method: CART and CIT

We compare our approach to two existing methods: CIT (Conditional Inference Trees) (Hothorn et al., 2006) and CART (Classification and Regression Trees) (Breiman et al., 2017). We selected these two methods because CART is well established and widely used, while CIT is conceptually closest to our method as it searches for correlations as well, though without the explicit search for functional relationships. Ensemble methods such as Random Forest (Breiman, 2001) are more complex realizations of the single tree methods used here but have the above discussed problems of interpretability, hence we do not include them here. MARS (Multivariate Adaptive Regression Splines) (Friedman, 1991) and other regression methods cannot separate domains in a hierarchical manner.

Using a greedy approach (A selection of the best possible option at a current state of the algorithm, thus possibly missing a global optimum), CART searches for an optimal binary split of a dataset that optimizes an error function such as the Gini index or an entropy measurement. CART trees tend to overfit and thus must be pruned for most datasets (Esposito et al., 1997). CIT is similar to CART as it constructs a binary tree and can produce regressions and classifications. However, to decide on a split CIT tests for a maximum linear independence between covariates and response variables. CIT stops if the null hypothesis H0 of variable's independence cannot be rejected. It selects a subset of the covariate with the highest conditional expectation using a linear two-sample test. CIT can be computationally expensive and was in the past used, e.g., to

176   determine the role of global change in soil functions (Rillig et al., 2019). It was, however,
177   criticized due to its limited ability for detecting non-linear effects (Wright et al., 2017).
178
179   In both CART and CIT trees, dominant controls are indicated by variables close to the tree's root
180   node. The earlier a variable is used for a split the more a separation improves the classification or
181   regression fit. Splits in SONAR provide a similar indication, however, controls also appear in the
182   leaf nodes. The controls selected in the leaf nodes may be equal to the ones used for a split or be
183   different.

184   2.3 Experimental setup

185   2.3.1 Groundwater recharge data and explanatory variables

186   We use groundwater recharge (see S1) as an example process to test the algorithms.
187   Groundwater recharge is poorly understood globally and available data are rather imbalanced
188   (Gnann et al., 2023a). For these reasons we use data produced by model simulation, rather than
189   observations. We also use a long-term estimate of recharge given that this is most likely related
190   to climatic factors which we consider here. Our dataset consists of simulated 30-year annual
191   averages of groundwater recharge on a 0.5° spatial resolution from an ensemble of eight global
192   hydrological models (Table S1) (Best et al., 2011; Burek et al., 2020; Gnann et al., 2023a;
193   Hanasaki et al., 2018; Müller Schmied et al., 2021; Schaphoff et al., 2018; Sutanudjaja et al.,
194   2018; Swenson & Lawrence, 2015; Takata et al., 2003). We investigate functional relationships
195   within the data to showcase differences between the algorithms. There is no intention here to
196   evaluate the specific model implementations or performances. For the classification task of
197   CART, we separate annual groundwater recharge amounts into four classes: very low (0-10
198   mm/yr), low (10-100 mm/yr), medium (100-500 mm/yr), and high (>500 mm/yr). Using
199   different separation categories does not change the general conclusions regarding the algorithms
200   but influences the specific CART trees (see Fig. S13). All models are driven with the same
201   forcing input (Table S2). Recharge simulations and forcing data are based on the simulation
202   protocol of the Inter-Sectoral Impact Model Intercomparison Project (ISIMIP) (Warszawski et
203   al., 2014).
204
205   In addition, we use a set of explanatory variables that we assume to be potentially relevant in
206   determining recharge in the eight models (Table S2 and Fig. S5-S9). We use long-term mean
207   precipitation (P), long-term mean potential evapotranspiration (PET), an aridity index (AI)
208   defined by PET/P, long-term mean temperature (T), an indicator of cold days per year (DB), and
209   a land cover data set GlobCover which is closest to the information used in the models (ESA,
210   2010). In contrast to common forcing, the hydrological models used consider very different
211   geological information which is therefore hard to consider here.
212
213   Traditionally machine learning methods are evaluated with established datasets like Iris (Unwin
214   & Kleinman, 2021) or Forest cover type (Jock Blackard, 1998), however they are either too
215   small to be used with SONAR or are built specifically for a classification problem which cannot
216   test the usefulness of approach.

217   2.4 Evaluation criteria of method attributes

218   2.4.1 Comparison between SONAR, CART and CIT

219   The three methods include different information in their leaf nodes and make very different split
220   decisions (see Section 2.2). To allow a general comparison, we compare the trees visually in
221   their pathways to derive at certain recharge classes (see 2.3.1). We focus on the dominant
222   controls (how far up in the tree explanatory variables are mentioned; see also 2.2), their
223   thresholds (split decisions), and the pathways that lead to certain value ranges. For the widely
224   used Iris dataset (Unwin & Kleinman, 2021) and a simple CART tree this path representation
225   shows that petal width is a dominant control (Fig. S14)
226
227   Since no other existing method represents functional relationships in their leaf nodes we use the
228   derived functional line of SONAR (see 2.1) to calculate ranges of values within the node (i.e.,
229   the range of possible Y for a given range of X) that can be compared to the regression and class
230   ranges of CART and CIT.

231   2.4.2 Robustness of SONAR

232   To test how SONAR reacts to data limitations we create a robustness test. A possible real-world
233   reason for this absence of data could be a sampling bias (e.g. Krabbenhoft et al. (2022)). Each
234   experiment removes a certain percentage of data from the original dataset at random. The less a
235   tree representation changes the more robust the algorithm is. This does not address the
236   correctness of the tree. We measure the robustness by utilizing the TED (tree-edit-distance)
237   (Pawlik & Augsten, 2015) defined as the minimum-cost sequence of node edit operations
238   (delete, insert, rename) that transform one tree into another. We use TED only to compare trees
239   derived within a method and not for cross-method comparison. In 100 independent experiments,
240   1 is the baseline experiment with all the available data, we randomly remove X% of the initial
241   data and compare the resulting tree to the baseline experiment. A method is more robust to
242   random removal of data if the TED remains small between the baseline and the 99 other
243   experiments. As a reference we compare the robustness of SONAR with the widely used CART
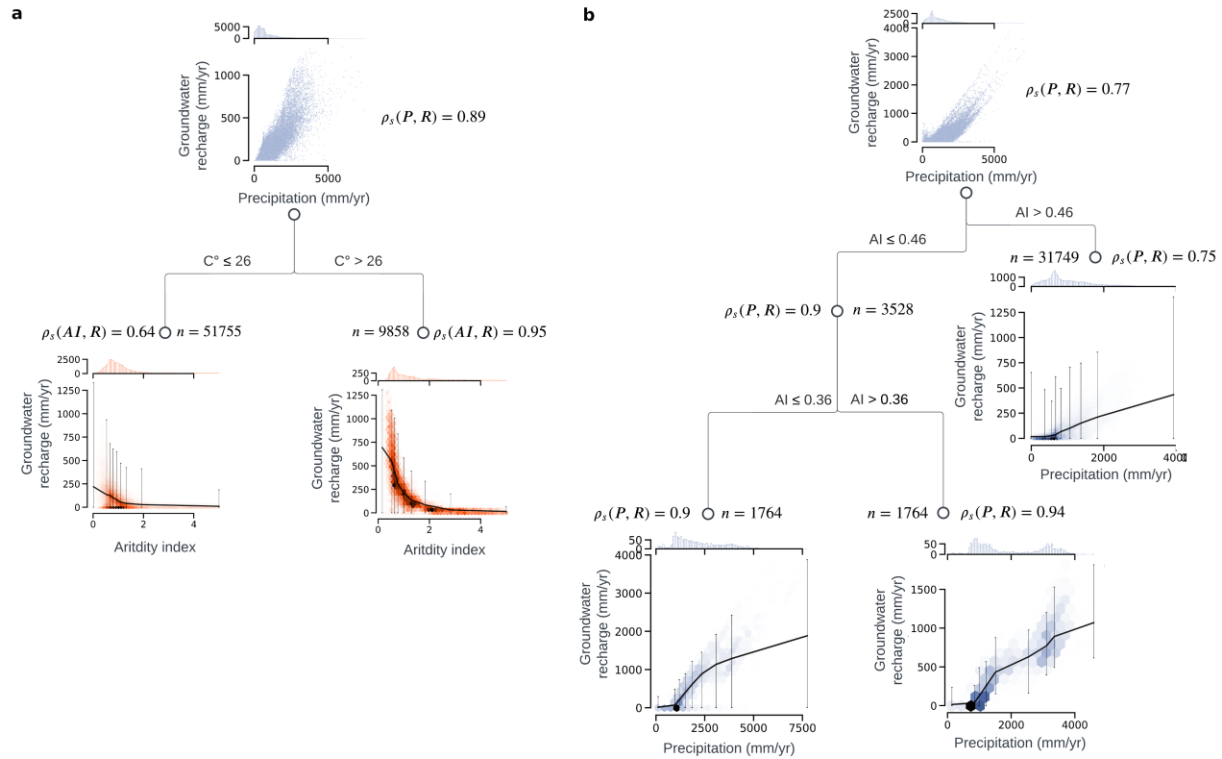244   method.

245   **3 Results**

246   3.1 Automatic detection of relationships in sub-domains using SONAR

247   Testing SONAR on groundwater recharge datasets from eight global hydrological models yields
248   eight different trees, two of which are shown in Fig. 2. We show models WaterGAP (Müller
249   Schmied et al., 2021) and LPJML (Schaphoff et al., 2018) (see also Table S1) as examples, while
250   all other models can be found in supplement S5. All resulting trees are rather shallow with only
251   one to four splits. This is a characteristic of SONAR that is amplified by the minimum number of
252   points requirement (see 2.1; without it the trees grow only marginally bigger, see supplement
253   S5).
254
255   SONAR finds highly correlated subsets of the data in its leafs with Spearman rank correlations p_s
256   > 0.9 (up to 0.95 for model (a) in Fig. 2a). Separation into different subspaces of the explanatory
257   variables, by temperature in Fig. 2a and by aridity index in Fig. 2b, together with the different

258 functional relationships in the leaf nodes, suggests that the global models WaterGAP and LPJML
259 differ in the way they represent groundwater recharge processes.
260
261 In Fig. 2a, the dominant control for the tree is the aridity index in all leaves; for the tree in Fig.
262 2b, it is precipitation. The fact that the same control appears in all leaves within a tree is specific
263 to these two trees, and different controls will be found across other datasets. Compared to the
264 initial correlation of 0.89 and 0.77 at the root node (both to precipitation), the correlation
265 increases for some subdomains but decreases for others. (SONAR only requires an increase in
266 one subdomain on a split, see 2.1). In our case study, the number of points in the highly
267 correlated domains is always much smaller than those in the less correlated domains and also
268 shows higher uncertainty in the functional relationships found (Fig. 2).
269

270
271 **Figure 2**. SONAR tree of models WaterGAP (a) and LPJML (b). n is the number of points at
272 each node, p_s the spearman correlation, the black line is the functional relationship, error bars
273 indicate the min. and max. value in each bin (here 10 quantiles). The color provides an indication
274 of the point density of the underlying data as a visual aid (lines and error bars are calculated
275 based on the underlying scatter of the original data). The darker the color the more points are
276 inside this area. The root shows the relationship between Precipitation (P) and Recharge (R)
277 because this shows the highest initial correlation in the data without splits.
278
279 To ensure that SONAR finds reasonable relationships we tested it with the same explanatory
280 variables and (1) randomly generated recharge, (2) recharge generated based on linear relations
281 to precipitation that differ for different domains, and (3) recharge generated based on PET (see
282 supplement). Using these examples, we show that SONAR does not produce any tree from
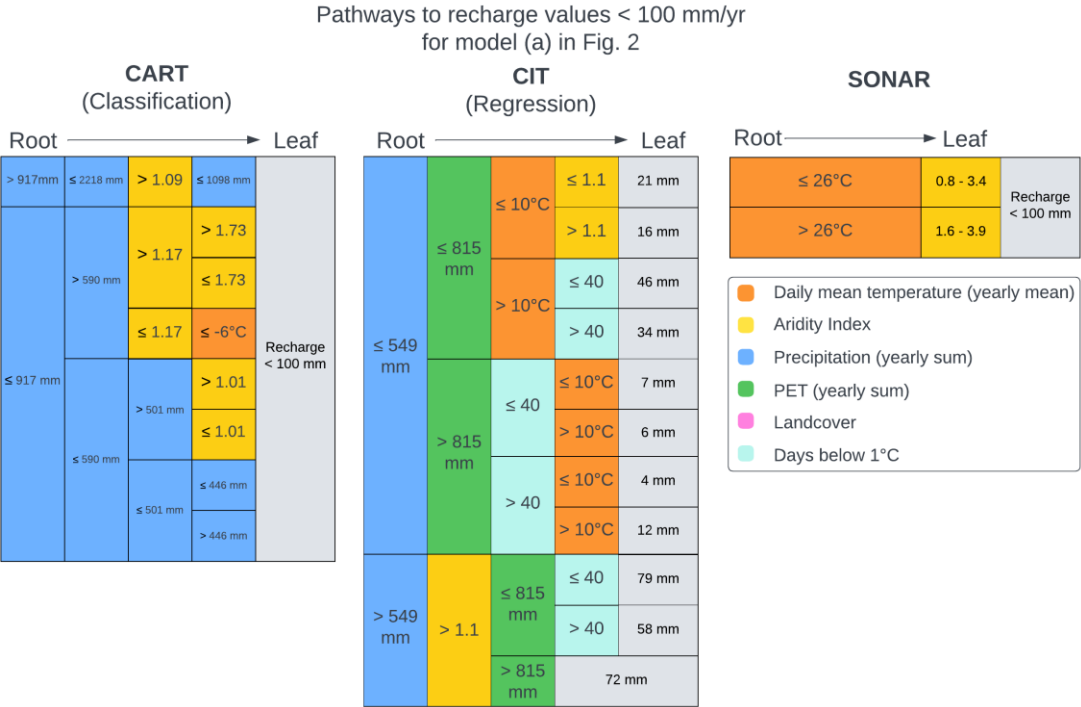
283   randomly generated data and is able to identify the artificial relationships for precipitation and
284   PET (see supplemental S7).

285   3.2 SONAR differs from CART and CIT in regression and classification paths

286   SONAR searches for functional relationships instead of classifications or regressions;
287   nevertheless, the meanings of the trees are similar enough to CART and CIT to compare the
288   interpretations and conclusions drawn. In Fig. 3, we represent sub-trees to enable such a
289   comparison (for a full explanation of the chosen visualization, see supplemental material),
290   including the results shown in Fig. 2a. For each tree, Fig. 3 only shows the part of the tree that
291   describes controlling variables on recharge values smaller than 100 mm/yr as an example (see
292   supplement Fig. S15, S16 for the complete trees). The visualization shows each path that leads to
293   a recharge value below or equal to 100 mm/yr, from the first split at the root node (left) to the
294   leaf node (right). A different box indicates a split, while the value and color inside the box
295   indicate at which point and through which variable the data was split. If a box is bigger, there are
296   more pathways and leaves following this split in the tree. The leaf shows only a single class for
297   classification trees (CART), values below the chosen threshold for regressions (CIT), and a
298   range of values within a functional relationship that produces values below the threshold
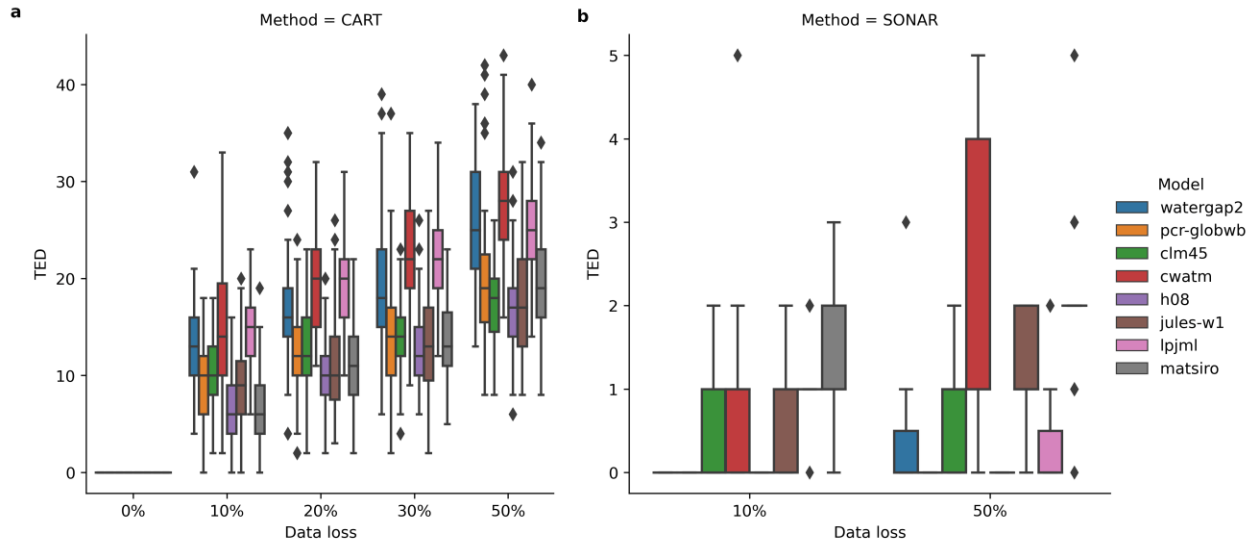299   (SONAR).
300
301   Equal to Fig. 2a the SONAR tree shows only one split at 26 C° in comparison to CART and CIT,
302   which show more possible pathways to low recharge values. All three approaches show different
303   dominant controls and pathways to low recharge values. The encoding of how low recharge
304   values are reproduced is much more complex in CART and CIT (multiple splits and different
305   variables that control them) and very short in SONAR. The CART tree suggests that
306   precipitation is the dominant control (as it shows up earlier in the tree) and that the aridity index
307   gets more important in certain subdomains. On the other hand, CIT also uses precipitation as the
308   first split but other explanatory variables for splitting the data further. Overall all three methods
309   differ substantially in their understanding of the data.

Figure 3. Visual representation of tree pathways (see supplement S4 for an extended explanation and simple example of this visualization method) only for low recharge values of three different approaches. The SONAR sub-plot shows part of Fig. 2a. For CART and CIT only, the part of the tree that leads to low values is shown. Gray boxes indicate the values or classes – for CIT and CART they are also the leaf nodes. All three trees were trained on the same model data and explanatory variables. The CART and CIT tree were pruned to a depth of 4.

3.3 SONAR is robust to variations in the input dataset

To test the robustness (see 2.4.2) of SONAR we removed a percentage of the original data and compared it with a baseline experiment. To provide a frame of reference we first conducted the experiment with the established CART algorithm (Fig. 4a). With an increased loss of information, the resulting CART trees become increasingly different (higher TED) from the baseline experiment which includes all data. Notably the mean difference between the models is relatively stable throughout. In comparison, SONAR is relatively robust as the TED with 10% loss is 1 magnitude smaller than with CART. Even with 50% of data loss SONAR only reaches a maximum TED of 5, for some models the tree does not change at all. Importantly, the small TED is likely highly impacted by the total size of the tree. SONAR leads to smaller trees to begin with.

Figure 4. Robustness test of CART (a) and SONAR (b). Bars show the distribution of TED over the 99 independent random experiments as an indicator for robustness (small values equal a smaller change from the original tree). If the there is no bar shown the TED is 0 and all trees are equal for that model.

4 Discussion and method limitations

The application of SONAR to simulated groundwater recharge of global hydrological models shows differences between models and overall precipitation as a strong control of recharge. Both of these findings alight with recent analysis of this data (Gnann et al., 2023a; West et al., 2023). Importantly, SONAR also reveals that precipitation is not always the strongest explanation for recharge variability (Fig. 1a shows aridity as functional control of recharge) and that relationships between precipitation and recharge may differ across data subsets (e.g., divided by climate as in Fig. 1b). As recharge is a complex process which is not only controlled by available water but also by e.g. soil conditions and energy availability, one should expect different functional relationships in different domains (e.g. climatic regions). Model developers could use the identified relationships to evaluate whether their model represents a functional relationship that is similar to our hydrologic understanding and data of a specific region.

The analysis reveals that SONAR produces very robust small trees but also differs largely in the path found towards small recharge values from very established algorithms. Importantly, because SONAR is so different from other algorithms (a search for functional relationships instead of regression or classification), a comparative analysis can only provide limited insights into whether it is more useful than established algorithms. SONAR results might allow for an easier discussion of their hydrological meaning compared to e.g. CART due to the smaller trees and relationships instead of discrete classes in its leaves.

We did not investigate observational data at this stage and we did not extend the analysis to the temporal domain, but there would not be any fundamental difference in workflow. An important aspect that needs further consideration is the role of epistemic uncertainty when applying SONAR to observational data. However, SONAR does not produce any tree from randomly

360   generated data (supplement S7) and is able to identify the artificially introduced relationships of
361   precipitation and PET (supplement S7). Wider analysis to other datasets will be required to
362   understand what relationships can be identified by SONAR.
363
364   The current implementation of SONAR has multiple limitations as we made specific
365   methodological choices. Foremost, we could have used another correlation metric (Lee Rodgers
366   & Nicewander, 1988), e.g., Pearson (Barber et al., 2020) instead of Spearman rank correlation.
367   Also, metrics that consider a degree of regression fit would be possible. Our current choices are
368   meant to require minimum assumptions. Furthermore, we chose to introduce a constraint on the
369   amount of points at which a split is carried out, to prevent the algorithm from creating very small
370   datasets in which the correlation calculation can become meaningless (see also S6). Selection of
371   meaningful subset of data is an active field of research thus other approaches in separating the
372   data at splits in SONAR could be considered (García-Pedrajas, 2011). And finally, the selection
373   of explanatory variables has an impact on the results for any type of empirical algorithm like the
374   one we present here, e.g. because variables like precipitation and aridity index are slightly
375   correlated (Fig. S12).
376

5 Conclusions

378   SONAR describes a new and simple approach to identify functional relationships in complex
379   datasets, thus giving effective insight into dominant controls within subdomains. The key
380   advantage of SONAR is the automatic, non-parametrized, representation of functional
381   relationships of hierarchical domains. It is specifically not built for classification or regression
382   tasks, but to find possible relationships in large datasets. A comparison to other tree approaches
383   shows that SONAR produces trees that are shorter and thus likely easier to interpret.
384   Furthermore, SONAR is very robust and does not require any parameter tuning to work on a
385   specific dataset.
386
387   Without any prior knowledge, SONAR enables researchers to explore vast datasets of model
388   simulations and observations to automatically discover exciting new functional relationships.
389   Especially in the field of hydrology, where controls differ largely across temporal and spatial
390   domains, we demonstrated that this new method can yield interesting new insights. Eventually
391   SONAR could also be used for model evaluation by enabling the comparison of functional
392   relationships identified in the data to those identified in model simulations.

403 **Open Research**

404 The original non-aggregated model data is available from isimip.org. The aggregated data is
405 available at Gnann et al. (2023b). A reference implementation of SONAR alongside with an
406 example use shown in this paper can be found at Reinecke (2023) and at
407 https://github.com/rreinecke/SONAR.

408 ## References

409 Almeida, S., Holcombe, E. A., Pianosi, F., & Wagener, T. (2017). Dealing with deep
410   uncertainties in landslide modelling for disaster risk reduction under climate change. *Natural*
411   *Hazards and Earth System Sciences*, *17*(2), 225–241. https://doi.org/10.5194/nhess-17-225-
412   2017

413 Antoniadis, A., Lambert-Lacroix, S., & Poggi, J.-M. (2021). Random forests for global
414   sensitivity analysis: A selective review. *Reliability Engineering & System Safety*, *206*,
415   107312. https://doi.org/10.1016/j.ress.2020.107312

416 Barber, C., Lamontagne, J. R., & Vogel, R. M. (2020). Improved estimators of correlation and R
417   2 for skewed hydrologic data. *Hydrological Sciences Journal*, *65*(1), 87–101.
418   https://doi.org/10.1080/02626667.2019.1686639

419 Berghuijs, W. R., Luijendijk, E., Moeck, C., van der Velde, Y., & Allen, S. T. (2022). Global
420   Recharge Data Set Indicates Strengthened Groundwater Connection to Surface Fluxes.
421   *Geophysical Research Letters*, *49*(23). https://doi.org/10.1029/2022GL099010

422 Best, M. J., Pryor, M., Clark, D. B., Rooney, G. G., Essery, R.. H., & Ménard, C. B., et al.
423   (2011). The Joint UK Land Environment Simulator (JULES), model description – Part 1:
424   Energy and water fluxes. *Geoscientific Model Development*, *4*(3), 677–699.
425   https://doi.org/10.5194/gmd-4-677-2011

426 Beven, K. J., Almeida, S., Aspinall, W. P., Bates, P. D., Blazkova, S., & Borgomeo, E., et al.
427   (2018). Epistemic uncertainties and natural hazard risk assessment – Part 1: A review of
428   different natural hazard areas. *Natural Hazards and Earth System Sciences*, *18*(10), 2741–
429   2768. https://doi.org/10.5194/nhess-18-2741-2018

430 Beven, K. J., & Cloke, H. L. (2012). Comment on "Hyperresolution global land surface
431   modeling: Meeting a grand challenge for monitoring Earth's terrestrial water" by Eric F.
432   Wood et al. *Water Resources Research*, *48*(1). https://doi.org/10.1029/2011WR010982

433 Bradter, U., Altringham, J. D., Kunin, W. E., Thom, T. J., O'Connell, J., & Benton, T. G. (2022).
434   Variable ranking and selection with random forest for unbalanced data. *Environmental Data*
435   *Science*, *1*. https://doi.org/10.1017/eds.2022.34

436 Breiman, L. (2001). Random forests. *Machine Learning*, *45*(1), 5–32.
437   https://doi.org/10.1023/A:1010933404324

438 Breiman, L., Friedman, J. H., Olshen, R. A., & Stone, C. J. (2017). *Classification And*
439   *Regression Trees*: Routledge.

440 Burek, P., Satoh, Y., Kahil, T., Tang, T., Greve, P., & Smilovic, M., et al. (2020). Development
441   of the Community Water Model (CWatM v1.04) – a high-resolution hydrological model for
442   global and regional assessment of integrated water resources management. *Geoscientific*
443   *Model Development*, *13*(7), 3267–3298. https://doi.org/10.5194/gmd-13-3267-2020

444 Chawla, N. V., Bowyer, K. W., Hall, L. O., & Kegelmeyer, W. P. (2002). SMOTE: Synthetic
445   Minority Over-sampling Technique. *Journal of Artificial Intelligence Research*, *16*, 321–357.
446   https://doi.org/10.1613/jair.953

447 Conoscenti, C., Ciaccio, M., Caraballo-Arias, N. A., Gómez-Gutiérrez, Á., Rotigliano, E., &
448   Agnesi, V. (2015). Assessment of susceptibility to earth-flow landslide using logistic
449   regression and multivariate adaptive regression splines: A case of the Belice River basin
450   (western Sicily, Italy). *Geomorphology*, *242*, 49–64.
451   https://doi.org/10.1016/j.geomorph.2014.09.020

452 Denissen, J. M. C., Teuling, A. J., Pitman, A. J., Koirala, S., Migliavacca, M., & Li, W., et al.
453   (2022). Widespread shift from ecosystem energy to water limitation with climate change.
454   *Nature Climate Change*, *12*(7), 677–684. https://doi.org/10.1038/s41558-022-01403-8

455 Eker, S., Rovenskaya, E., Obersteiner, M., & Langan, S. (2018). Practice and perspectives in the
456   validation of resource management models. *Nature Communications*, *9*(1), 5359.
457   https://doi.org/10.1038/s41467-018-07811-9

458 ESA. (2010). Global land cover map. Retrieved from http://due.esrin.esa.int/page_globcover.php

459 Esposito, F., Malerba, D., Semeraro, G., & Kay, J. (1997). A comparative analysis of methods
460   for pruning decision trees. *IEEE Transactions on Pattern Analysis and Machine Intelligence*,
461   *19*(5), 476–493. https://doi.org/10.1109/34.589207

462 Friedman, J. H. (1991). Multivariate Adaptive Regression Splines. *The Annals of Statistics*,
463   *19*(1). https://doi.org/10.1214/aos/1176347963

464 García-Pedrajas, N. (2011). Evolutionary computation for training set selection. *Wiley
465   Interdisciplinary Reviews: Data Mining and Knowledge Discovery*, *1*(6), 512–523.
466   https://doi.org/10.1002/widm.44

467 Gnann, S., Reinecke, R., Stein, L., Wada, Y., Thiery, W., & Müller Schmied, H., et al. (2023a).
468   Functional relationships reveal differences in the water cycle representation of global water
469   models. Preprint (accepted in Nature Water). https://doi.org/10.31223/X50S9R

470 Gnann S., Reinecke, R. et al. (2023b). Data to "Functional relationships reveal differences in the
471   water cycle representation of global water models" [Data set]. Zenodo.
472   https://doi.org/10.5281/zenodo.7714885

473 Hanasaki, N., Yoshikawa, S., Pokhrel, Y., & Kanae, S. (2018). A global hydrological simulation
474   to specify the sources of water used by humans. *Hydrology and Earth System Sciences*, *22*(1),
475   789–817. https://doi.org/10.5194/hess-22-789-2018

476 Hoch, J. M., Sutanudjaja, E. H., Wanders, N., van Beek, R. L. P. H., & Bierkens, M. F. P.
477   (2023). Hyper-resolution PCR-GLOBWB: opportunities and challenges from refining model
478   spatial resolution to 1 km over the European continent. *Hydrology and Earth System Sciences*,
479   *27*(6), 1383–1401. https://doi.org/10.5194/hess-27-1383-2023

480 Hothorn, T., Hornik, K., & Zeileis, A. (2006). Unbiased Recursive Partitioning: A Conditional
481   Inference Framework. *Journal of Computational and Graphical Statistics*, *15*(3), 651–674.
482   https://doi.org/10.1198/106186006X133933

483 Jiang, S., Bevacqua, E., & Zscheischler, J. (2022). River flooding mechanisms and their changes
484   in Europe revealed by explainable machine learning. *Hydrology and Earth System Sciences*,
485   *26*(24), 6339–6359. https://doi.org/10.5194/hess-26-6339-2022

486 Jock Blackard. (1998). *Covertype.* https://doi.org/10.24432/C50K5N

Kaur, H., Pannu, H. S., & Malhi, A. K. (2020). A Systematic Review on Imbalanced Data Challenges in Machine Learning. *ACM Computing Surveys*, *52*(4), 1–36. https://doi.org/10.1145/3343440

Koster, R. D., & Milly, P. C. D. (1997). The Interplay between Transpiration and Runoff Formulations in Land Surface Schemes Used with Atmospheric Models. *Journal of Climate*, *10*(7), 1578–1591. https://doi.org/10.1175/1520-0442(1997)010<1578:TIBTAR>2.0.CO;2

Krabbenhoft, C. A., Allen, G. H., Lin, P., Godsey, S. E., Allen, D. C., & Burrows, R. M., et al. (2022). Assessing placement bias of the global river gauge network. *Nature Sustainability*, *5*, 586–592. https://doi.org/10.1038/s41893-022-00873-0

Lee Rodgers, J., & Nicewander, W. A. (1988). Thirteen Ways to Look at the Correlation Coefficient. *The American Statistician*, *42*(1), 59–66. https://doi.org/10.1080/00031305.1988.10475524

Lesk, C., Coffel, E., Winter, J., Ray, D., Zscheischler, J., Seneviratne, S. I., & Horton, R. (2021). Stronger temperature-moisture couplings exacerbate the impact of climate warming on global crop yields. *Nature Food*, *2*(9), 683–691. https://doi.org/10.1038/s43016-021-00341-6

Loh, W.-Y. (2014). Fifty Years of Classification and Regression Trees. *International Statistical Review*, *82*(3), 329–348. https://doi.org/10.1111/insr.12016

L'vovich, M. I. (1979). *World Water Resources and Their Future*. Washington, D. C.: American Geophysical Union.

MacDonald, A. M., Lark, R. M., Taylor, R. G., Abiye, T., Fallas, H. C., & Favreau, G., et al. (2021). Mapping groundwater recharge in Africa from ground observations and implications for water security. *Environmental Research Letters*, *16*(3), 34012. https://doi.org/10.1088/1748-9326/abd661

Messager, M. L., Lehner, B., Cockburn, C., Lamouroux, N., Pella, H., & Snelder, T., et al. (2021). Global prevalence of non-perennial rivers and streams. *Nature*, *594*(7863), 391–397. https://doi.org/10.1038/s41586-021-03565-5

Müller Schmied, H., Cáceres, D., Eisner, S., Flörke, M., Herbert, C., & Niemann, C., et al. (2021). The global water resources and use model WaterGAP v2.2d: model description and evaluation. *Geoscientific Model Development*, *14*(2), 1037–1079. https://doi.org/10.5194/gmd-14-1037-2021

NASA. (2021). NASA turns to the cloud for help with next generation earth missions. Retrieved from https://www.jpl.nasa.gov/news/nasa-turns-to-the-cloud-for-help-with-next-generation-earth-missions

Pattee, H. H. (1972). Chapter 1 - THE NATURE OF HIERARCHICAL CONTROLS IN LIVING MATTER. In R. Rosen (Ed.), *Foundations of Mathematical Biology* (pp. 1–22). Academic Press. https://doi.org/10.1016/B978-0-12-597201-7.50008-5

Pawlik, M., & Augsten, N. (2015). Efficient Computation of the Tree Edit Distance. *ACM Transactions on Database Systems*, *40*(1), 1–40. https://doi.org/10.1145/2699485

Peterson, T. J., Saft, M., Peel, M. C., & John, A. (2021). Watersheds may not recover from drought. *Science (New York, N.Y.)*, *372*(6543), 745–749. https://doi.org/10.1126/science.abd5085

528 Pianosi, F., & Wagener, T. (2018). Distribution-based sensitivity analysis from a generic input-
529   output sample. *Environmental Modelling & Software*, *108*, 197–207.
530   https://doi.org/10.1016/j.envsoft.2018.07.019

531 Puy, A., Roy, P. T., & Saltelli, A. (2022). *Discrepancy measures for sensitivity analysis*.
532   Retrieved from http://arxiv.org/pdf/2206.13470v2

533 Reichstein, M., Camps-Valls, G., Stevens, B., Jung, M., Denzler, J., Carvalhais, N., & Prabhat.
534   (2019). Deep learning and process understanding for data-driven Earth system science.
535   *Nature*, *566*(7743), 195–204. https://doi.org/10.1038/s41586-019-0912-1

536 Reinecke, R. (2023) SONAR (v.0.1). Zenodo. https://doi.org/10.5281/zenodo.10008510

537 Reinecke, R., Müller Schmied, H., Trautmann, T., Andersen, L. S., Burek, P., & Flörke, M., et
538   al. (2021). Uncertainty of simulated groundwater recharge at different global warming levels:
539   a global-scale multi-model ensemble study. *Hydrology and Earth System Sciences*, *25*(2),
540   787–810. https://doi.org/10.5194/hess-25-787-2021

541 Rillig, M. C., Ryo, M., Lehmann, A., Aguilar-Trigueros, C. A., Buchert, S., & Wulf, A., et al.
542   (2019). The role of multiple global change factors in driving soil functions and microbial
543   biodiversity. *Science (New York, N.Y.)*, *366*(6467), 886–890.
544   https://doi.org/10.1126/science.aay2832

545 Saltelli, A., Jakeman, A., Razavi, S., & Wu, Q. (2021). Sensitivity analysis: A discipline coming
546   of age. *Environmental Modelling & Software*, *146*, 105226.
547   https://doi.org/10.1016/j.envsoft.2021.105226

548 Sarailidis, G., Wagener, T., & Pianosi, F. (2023). Integrating scientific knowledge into machine
549   learning using interactive decision trees. *Computers & Geosciences*, *170*, 105248.
550   https://doi.org/10.1016/j.cageo.2022.105248

551 Schaphoff, S., Bloh, W. von, Rammig, A., Thonicke, K., Biemans, H., & Forkel, M., et al.
552   (2018). LPJmL4 – a dynamic global vegetation model with managed land – Part 1: Model
553   description. *Geoscientific Model Development*, *11*(4), 1343–1375.
554   https://doi.org/10.5194/gmd-11-1343-2018

555 Sheikholeslami, R., & Razavi, S. (2020). A Fresh Look at Variography: Measuring Dependence
556   and Possible Sensitivities Across Geophysical Systems From Any Given Data. *Geophysical
557   Research Letters*, *47*(20). https://doi.org/10.1029/2020GL089829

558 Shrestha, D. L., Kayastha, N., & Solomatine, D. P. (2009). A novel approach to parameter
559   uncertainty analysis of hydrological models using neural networks. *Hydrology and Earth
560   System Sciences*, *13*(7), 1235–1248. https://doi.org/10.5194/hess-13-1235-2009

561 Sutanudjaja, E. H., van Beek, R., Wanders, N., Wada, Y., Bosmans, J. H. C., & Drost, N., et al.
562   (2018). PCR-GLOBWB 2: a 5 arcmin global hydrological and water resources model.
563   *Geoscientific Model Development*, *11*(6), 2429–2453. https://doi.org/10.5194/gmd-11-2429-
564   2018

565 Swenson, S. C., & Lawrence, D. M. (2015). A GRACE -based assessment of interannual
566   groundwater dynamics in the C ommunity L and M odel. *Water Resources Research*, *51*(11),
567   8817–8833. https://doi.org/10.1002/2015WR017582

568 Takata, K., Emori, S., & Watanabe, T. (2003). Development of the minimal advanced treatments
569   of surface interaction and runoff. *Global and Planetary Change*, *38*(1-2), 209–222.
570   https://doi.org/10.1016/S0921-8181(03)00030-4

571 Unwin, A., & Kleinman, K. (2021). The Iris Data Set: In Search of the Source of Virginica.
572   *Significance*, *18*(6), 26–29. https://doi.org/10.1111/1740-9713.01589

573 Wagener, T., & Kollat, J. (2007). Numerical and visual evaluation of hydrological and
574   environmental models using the Monte Carlo analysis toolbox. *Environmental Modelling &*
575   *Software*, *22*(7), 1021–1033. https://doi.org/10.1016/j.envsoft.2006.06.017

576 Wagener, T., Reinecke, R., & Pianosi, F. (2022). On the evaluation of climate change impact
577   models. *WIREs Climate Change*, *13*(3). https://doi.org/10.1002/wcc.772

578 Warszawski, L., Frieler, K., Huber, V., Piontek, F., Serdeczny, O., & Schewe, J. (2014). The
579   Inter-Sectoral Impact Model Intercomparison Project (ISI-MIP): project framework.
580   *Proceedings of the National Academy of Sciences of the United States of America*, *111*(9),
581   3228–3232. https://doi.org/10.1073/pnas.1312330110

582 West, C., Reinecke, R., Rosolem, R., MacDonald, A. M., Cuthbert, M. O., & Wagener, T.
583   (2023). Ground truthing global-scale model estimates of groundwater recharge across Africa.
584   *The Science of the Total Environment*, *858*(Pt 3), 159765.
585   https://doi.org/10.1016/j.scitotenv.2022.159765

586 Wright, M. N., Dankowski, T., & Ziegler, A. (2017). Unbiased split variable selection for
587   random survival forests using maximally selected rank statistics. *Statistics in Medicine*, *36*(8),
588   1272–1284. https://doi.org/10.1002/sim.7212

589 Zehe, E., & Sivapalan, M. (2009). Threshold behaviour in hydrological systems as (human) geo-
590   ecosystems: manifestations, controls, implications. *Hydrology and Earth System Sciences*,
591   *13*(7), 1273–1297. https://doi.org/10.5194/hess-13-1273-2009

592